

Integrating seismic refraction and electrical approaches in determining geophysical properties of near-surface cavities in Calabar-Ikom highway, Odukpani, Cross River State, Nigeria

Bassey Ukorebi Asuquo¹, Anthony M. George², Emmanuel Akaerue², Obinna Chigoziem Akakuru^{3*}

¹Department of Physics, Cross River University of Technology, Calabar, Cross River State, Nigeria

²Department of Physics, University of Calabar, Calabar, Cross River State, Nigeria

³Department of Geology, Federal University of Technology Owerri, Owerri West Nigeria

*Corresponding author E-mail: obinna.akakuru@futo.edu.ng

Abstract

Integrated seismic refraction tomography (SRT) and electrical resistivity tomography (ERT) were used to study near-surface cavities with the aim of determining their geophysical properties. Five seismic refraction profiles around the study area were carried out using a 24-channel seismograph (ES-3000) while four ERT and ERT profiles were also conducted with IGIS resistivity meter and PLOTREFA software respectively. The data was processed using the RES2DINV software. Travel-time curves and velocity models were generated from the processed SRT data for each survey line, and 2-D inverted apparent resistivity models along the same lines were also generated for the purpose of comparison respectively. The results as obtained from the profiles showed SRT 1 (with a modelled velocity of 1,216 m/s in layer two at a depth of approximately 11 m - 20 m beneath the subsurface and an estimated cavity diameter of 11 m) and ERT 1 (with an apparent resistivity of approximately 826 Ω m and a depth of approximately 12.5 m - 16 m) indicates that the near-surface cavity outcrop links with a close-by mountainous structure in the EW direction. Profiles SRT 2 (with an approximately modeled velocity layer of 980 m/s in layer two at an approximate depth of 3.5 m - 7.0 m) and SRT 3 (with a modeled velocity layer of approx. 1,000 m/s in layer two at an approximate depth of 4.0 m - 7.0 m and 3.0 m - 9.0 m); ERT 2 (with an apparent resistivity of approximately 80 Ω m); and ERT 3 (with apparent resistivities of 116 Ω m and 182 Ω m at depths of approximately 3.5 m to 6.4 m and 4.0 m to 15.8 m) indicates that the surface cavity outcrop extends underneath the road network (Odukpani Central Section of Calabar-Ikom Highway) with a width of approximately 12 m. Profiles SRT 4 and SRT 5 (with an average velocity layer of 1,000 m/s in layer two at an approximate depth of 6.0 m - 13.2 m), and ERT 4 (with apparent resistivity ranging between 121 Ω m and 172 Ω m) at a depth of approximately 9.5 m to 20.0 m reveal that the near-surface cavity extends up to about 11 m across the highway and about 120 m away from the edge of the road. The above result will serve as reliable technical information to Transport and Building Construction Engineers on the presence of cavities along road networks and settlement areas in Odukpani Local Government Area. The recommendation is also made for the use of other geophysical techniques like Ground Penetration Radar (GPR) in conjunction with SRT and ERT to get higher-resolution imagery of the study area.

Keywords: Near-Surface Cavities; Geophysical Properties; Seismic Refraction Tomography; Electrical Resistivity Tomography; Karst, Road Failures.

1. Introduction

The presence of undetected shallow subsurface cavities poses environmental and engineering risks if action is not taken to mitigate its presence. Cavities, voids, caves, caverns, karst, and sinkholes are all subsurface landforms that are referred to as subsurface cavities. When carbonates (such as dolomite and limestone) disintegrate and then evaporate, they produce the most prevalent natural voids (e.g., gypsum, salt, and anhydrite) (Metwaly & AlFouzan, 2013) The major concern posed by the presence of these subsurface cavities is the risk of ground surface subsidence arising from the slow migration of fine particles. This ground surface subsidence, if occurring along major road networks, could greatly damage property and loss of life. Construction and maintenance of good roads and highway networks in Cross River State has become a major problem. The worst thing is that even the newly constructed roads experience failures at different sections in less than six months or within a year. There is great concern about the rate of failure of these roads because a huge amount of money has been spent on the construction of such roads; hence the need for proper care to be taken geologically before roads and buildings are constructed. Subsidence on the road indicates that the underlying pavement structure is deteriorating (Eyankware et al. 2022a,b,c & d; Chizoba et al 2023; Obasi 2020).

Due to the widespread extent of road collapse over the nation's outdated transportation system, full-scale rehabilitation of every location is both expensive and often impossible. Subsidence can be caused by a number of factors. Some processes, such as huge void creation and

sinkhole formation, can result in rapid and catastrophic pavement failure, whereas others, such as delayed movement of small particles from the subgrade, might result in seasonal or gradual sinking. In karstic conditions, porous surface rocks are perfect for the formation of dangerous voids, and eventual ground subsidence, leading to a significant impact on civil (structural) engineering (De Giorgi & Leucci, 2014; Opara et al. 2022; 2023; Urom et al. 2021; Omoko et al. 2023). However, field observations and laboratory research have demonstrated that a lack of understanding of the composition and behaviour of subsoils on which roads are constructed on could be a major contributor to road failures (Ajayi, 1987). Pre-existing geological structures such as fractures and faults, the existence of shear zones and old stream channels, near-surface geologic succession, and the nature of soil surface (subgrade), have all been proved to be geologic hazards that can compromise any road's structural stability. As a result, prior to any road development, these elements must be thoroughly evaluated (Adiat et al., 2017; Oli et al 2022; Agidi et al. 2022; Akakuru et al. 2023a,2023b, 2023c).

Applying geophysical techniques in delineating shallow features can never be overemphasized. However, the problem has always been to determine the most appropriate geophysical technique to apply. This problem usually arises from unpredictable changes in subsurface features and the limitations of different geophysical methods. The goals of certain subsurface investigations as explained by Burger et al., (2006) are impossible to attain with a single geophysical method. This is due to the shortcomings and uncertainties of employing a single approach, such as noise, resolution, and a lack of sufficient contrast in physical qualities, which might limit geophysical methods in various situations.

In recent times, ERT has become a common technique for exploring the subsurface in karst formations due to the huge contrast in resistivity between air-fill voids and the underlying strata. The resistivity is high when the void features are dried; however, as the voids are filled with clay or water, the resistivity drops (Jaafar, 2017). There are numerous electrode configurations for two-dimensional ERT surveys including dipole-dipole, Schlumberger, pole-dipole, and Wenner. The degree to which these arrays are sensitive to vertical or horizontal variances, as well as the impact of noise, all play a part in understanding which of the above configurations could offer a good outcome in cavity features. Failure to use geophysical approaches in highway and building construction has led to the loss of structural integrity of said structures (Jaafar, 2017).

A subsequent geophysical technique used in interpreting seismic refraction data is seismic refraction tomography (SRT). SRT uses an inversion approach to determine the velocity of three-dimensional and two-dimensional models. The object is divided into cells known as voxels in 3-D and pixels in 2-D by the tomography concept. The initial model is tweaked to reduce the discrepancy between the computed and real travel times. The final model is established as soon as the least root-mean-square (RMS) error or the misfit value is obtained (Bery, 2013).

Many researchers have used integrated geophysical techniques to investigate and delineate areas with the presence of subsurface cavities. In the city of Rome, Cardarelli et al., (2010) conducted a study by combining ERT and SRT data in a collaborative interpretation procedure for cavity detection. Samyn et al., (2014) used an integrated geophysical technique that included MASW and ERT to analyze the occurrence of karst and sinkhole susceptibility along flood-protection dykes of the Loire River, Orléans, France. Araffa et al. (2014) explored the subsurface of Quarter 27 of May 15th City, Cairo, Egypt to demarcate the contamination, measure some aquifer parameters, and detect buried objects. Using two distinct electrode configurations, eight 2-D ERT sections were captured (dipole-dipole and Wenner). Rodriguez et al., (2020) employed electrical resistivity tomography (ERT) to discover subsurface cavities generated by underground coal mining in the carboniferous area of Coahuila, Mexico, as well as the threats they pose. In three mining-related zones, measurements were collected close to road and bridge support. Ilori et al., (2014) performed an investigation of highway pavement collapse at various places on some routes in southern Nigeria.

This research is aimed at determining the geophysical features of near-surface cavities in the Odukpani Central section of Calabar-Ikom Highway, Cross River State through the use of SRT and ERT with the following objectives: acquire P-wave arrival times; acquire apparent resistivity values; derive velocity-depth profiles of P-wave velocities (vertical seismic profiles); plot apparent resistivity profiles (tomographs); estimate the depth, and lateral extent of the cavities from the models obtained; and determine the dimensions of the cavities. Geophysics plays a significant role in site characterization and as a result, this research will have an enormous impact once accomplished. The result of this study will provide reliable technical information to transport Engineers (those in charge for planning, designing, and supervising the building and maintenance of civil engineering projects relating to transportation networks, such as bridges, roads, railways, mass transit stations, etc.) and Building Construction Engineers on the presence of voids/caves along road networks and settlement areas in Odukpani Local Government Area.

This study generally will help to infer if the near-surface cave extends under the highway (Odukpani Central Section of Calabar-Ikom Highway) crossing the study area and its surrounding environs. If this observation is positive, it will serve as a warning signal to applicable road users, and to the government to immediately commence maintenance work on the affected area/section of the highway.

2. Materials and method

2.1. The study area

The study area is located within Odukpani Central in Odukpani Local Government Area (LGA), Cross River State. It lies between latitude 5°07'0" N and 5°10'0" N, and longitude 8°18'0" E and 8°22'0" E (Fig. 1).

Geologically, Odukpani is underlain by the Calabar Flank which belongs to the Southern section of the Nigerian Sedimentary Basin which has the Oban Massif at its northern borders, and the Calabar hinge-line marking the Niger Delta basin at its southern borders. The NE-SW trending fault separates it to the west from the Ikpe Basin. It reaches the Cameroon Volcanic Ridge in the east (Ilori, 2016). Stratigraphically, the Odukpani Group of Cretaceous strata is made up of mid-albian to early cenomanian mfamosing limestone formation with a continuous thick grey-black, carbonaceous cenomanian Ekenkpong Shale (Petters et al, 1995). On top of this lies the New Netim Marl (thick coniacian, calcareous). The carbonaceous black Nkporo Shale lies unconformably on top of it (Reyment, 1965) (Fig. 2).

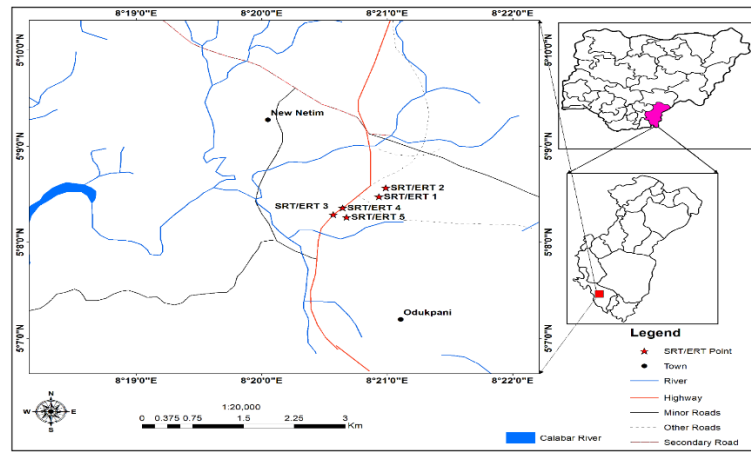


Fig. 1: Location Map of the Study Area (ArcGIS, 2016).

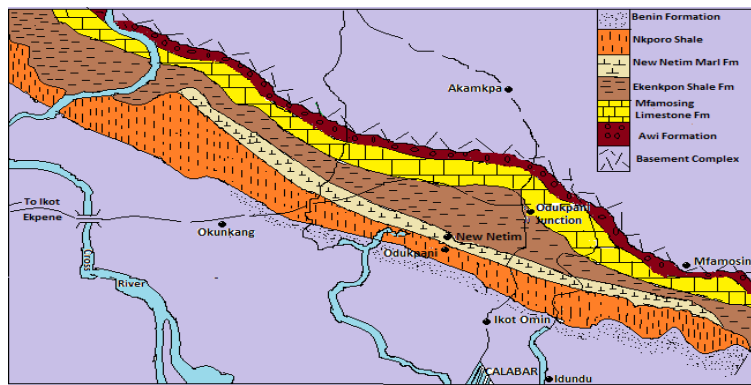


Fig. 2:

Table 1: Velocity Ranges of Earth Materials (United States Bureau of Reclamation, 2002)

Material	Velocity (feet per second)	(meters per second)
Moist fine-grained topsoil, sand, loam, loose gravel, dry silt, loose rock, and talus	600 - 2,500	200 - 800
Indurated clays, compact till, gravel below water table*, sand, compact clayey gravel, and sand-clay	2,500 - 7,500	800 - 2,300
Fractured, weathered, or partly decomposed rock	2,000 - 10,000	600 - 3,000
Sound limestone, chalk	6,000 - 20,000	2,000 - 6,100
Sound sandstone	5,000 - 14,000	1,500 - 4,000
Sound shale	2,500 - 11,000	800 - 3,400
Sound metamorphic rock	10,000 - 16,000	3,100 - 4,900
Sound igneous rock	12,000 - 20,000	3,700 - 6,100
*Water (saturated materials should have velocities equal to or exceeding that of water)	4,700	1,400

The following equipment were employed to conduct the SRT survey: a multi-channel seismograph (Geometrics ES-3000 Seismograph 24-channel); Receivers (24 P-wave geophones); Seismic source (sledgehammer and a base plate); Measuring tape; Transmitting cables; Battery (12V); Global Positioning System (GPS) and laptop computer; survey crew (cable hustlers).

The following equipment were employed to conduct the ERT survey: A multi-channel resistivity meter (IGIS Resistivity Meter); Electrodes; Transmitting cable reels; Hammer; DC Power Source; and Measuring tape.

Using the in-line refraction profiling approach, seismic refraction tomography (SRT) data were gathered along profiles that are approximately close to locations of near-surface caves. The measurements' main purpose was to figure out the compressional wave velocities of ground conditions as well as the depth to bedrock at five distinct profiles across the research region.

To record seismic data, twenty-four 10 Hz geophones were strung up in a straight line following prescribed profiles (Appendix 1) and linked to the seismograph. As an acoustic (energy) source, a 12 kg sledgehammer and a metal plate were used to create waves that were recorded by geophones (serving as receivers) as a function of time. Seismic refraction data were then acquired for each location. The profile length at each location was 69 m with inter geophone spacing of 3 m with an offset of 5 m from the first geophone. Data were collected in both forward and reverse direction.

An Integrated Geo Instruments and Services (IGIS) resistivity meter was used to collect ERT data along four of the five SRT profiles (model SSR-MP-ATS). Along the collected profiles, a Wenner electrode design was employed with a unit electrode spacing of 5 m – 35 m. The multiple electrode technique was used to accommodate the chosen profile length while also maintaining reasonable underground lateral resolution.

Twenty-two (22) electrodes were inserted into the ground at equal distances apart to cover the proposed profile length and maintain reasonable subsurface lateral resolution (Plate 1). The total profile length for ERT 1 was 120 m while ERT 2, ERT 3, and ERT 4 had a profile length of 105 m. The unit electrode spacing (a) ranging from 5 m, 10 m, 15 m, 20 m, 25 m, 30 m, and 35 m were used to measure seven segments of each of the four ERT profiles (Appendix 1) respectively.



Plate 1: Image Showing Field Data Acquisition.

3. Results and discussion

The acquired SRT data were processed and interpreted using SeisImager, a seismic interpretation software suite that includes software package such as Pickwin Version 4.4.1.0, and Plotrefa Version 2.9.2.6, etc. To produce time-distance curves, the first stage involves accurately choosing the initial breaks from the seismic signal for P-wave using the Pickwin software for each shot record. The time-distance curves were then created using the first arrival time, survey line distance, source location, and geophone spacing as inputs. Modelling the velocity-depth profiles from the recorded seismic velocity by appending the chosen initial breaks and generating a tomographic inversion of the velocity-depth model were the second and third stages of processing, respectively, using the Plotrefa program.

RES2DINV inversion software's concatenate function was used to combine the individual segments of each of the four ERT profiles into a single profile. For Wenner setup, the apparent resistivity was calculated as the product of resistance and the geometric factor. To compare the data and detect sedimentary boundaries, smooth and robust inversions were used. The data collected during field measurements of ERT is traditionally presented as pseudo-sections of apparent resistivity, which provide a rough estimate of subsurface resistivity. A baseline model was developed based on a priori data from averaged geophysical data gathering, and apparent resistivity data was modelled according to the survey geometry. The computed data was compared to field measurements, and the model was adjusted to account for the discrepancy between observed and estimated findings. This process was repeated until the produced data matched the real readings within a certain margin of error. The inversion technique results in a more accurate depth estimate for cross-section plots, transforming pseudo-sections into accurate estimates of subsurface variation.

Analysed travel-time curves and corresponding velocity models for each of the SRT profiles (SRT 1 – SRT 5) are presented as shown in FIGS 3 – 12. The results as obtained from the profiles revealed SRT 1 with four layers having modelled P-wave velocities of 300 ms^{-1} for the first layer, $1,216 \text{ ms}^{-1}$ for second layer, $1,895 \text{ ms}^{-1}$ for the third layer, and $3,000 \text{ ms}^{-1}$ for the fourth layer (FIG. 4). SRT 2 revealed three layers with modelled V_P of 300 ms^{-1} for the first layer, 980 ms^{-1} for the second layer, and $3,000 \text{ ms}^{-1}$ for third layer (see FIG. 6). Three layers were delineated from the results of profile SRT 3 with modelled V_P of 300 ms^{-1} for the first layer, $1,000 \text{ ms}^{-1}$ for the second layer, and $2,000 \text{ ms}^{-1}$ for the third layer (FIG. 8). SRT 4 and SRT 5 shared the same traverse end-to-end revealing three layers with average modelled V_P of 300 ms^{-1} for first layer, $1,000 \text{ ms}^{-1}$ for the second layer, and $2,000 \text{ ms}^{-1}$ for the third layer (FIG. 10 and FIG. 12).

From the modelled velocity profiles for SRT 1 – 5, near surface caves were inferred on layer two at an approximate depth of $11.0 \text{ m} - 20.0 \text{ m}$; layer two at an approximate depth of $3.5 \text{ m} - 7.0 \text{ m}$, layer two at an approximate depth of $4.0 \text{ m} - 7.0 \text{ m}$ and $3.0 \text{ m} - 9.0 \text{ m}$; layer two at an approximate depth of $0 \text{ m} - 13.2 \text{ m}$; and layer two at an approximate depth of $6.0 \text{ m} - 13.2 \text{ m}$ respectively.

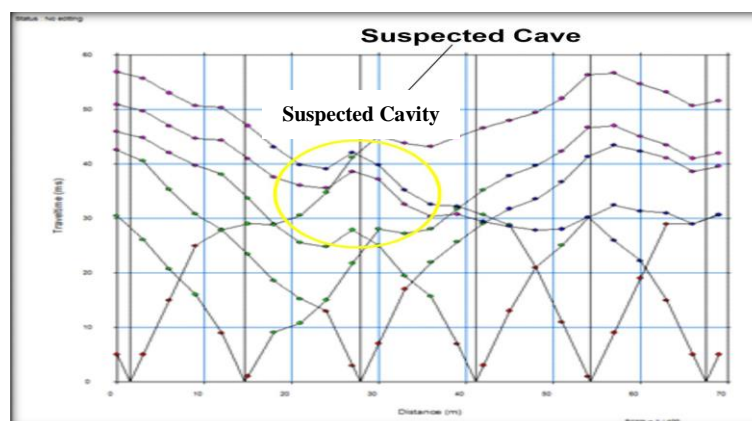


Fig. 3: Travel-Time Curve for SRT 1.

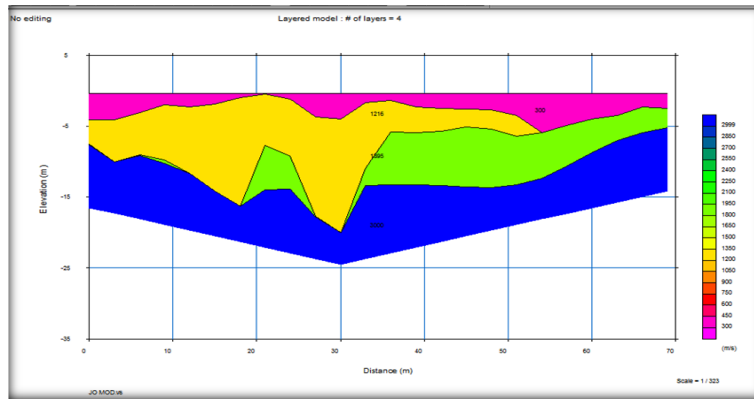


Fig. 4: Velocity Model for SRT 1.

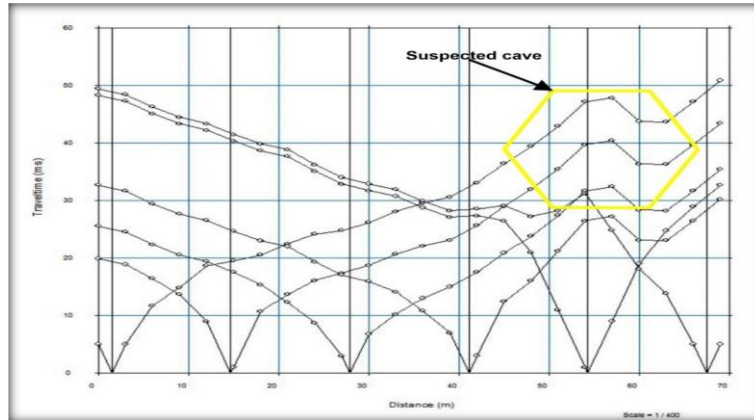


Fig. 5: Travel-Time Curve for Srt 2.

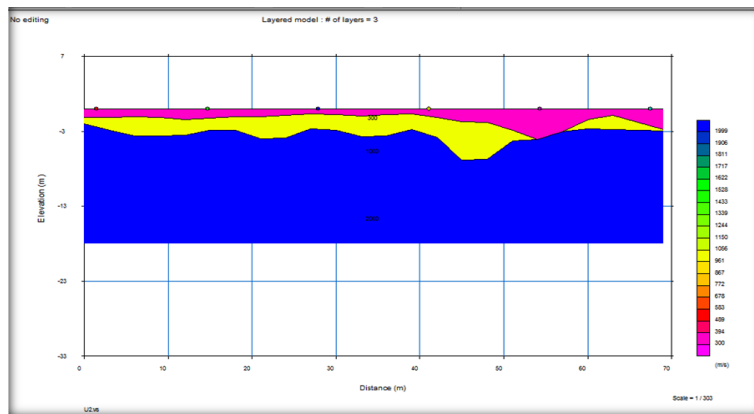


Fig. 6: Velocity Model for SRT 2.

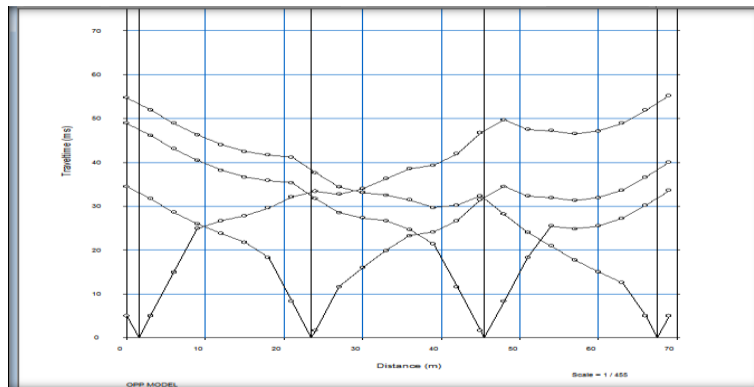


Fig. 7: Travel-Time Curve for Srt 3.

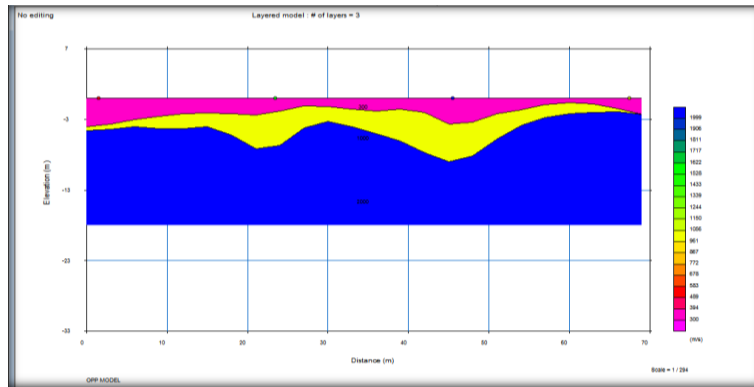


Fig. 8: Velocity Model for Srt 3.

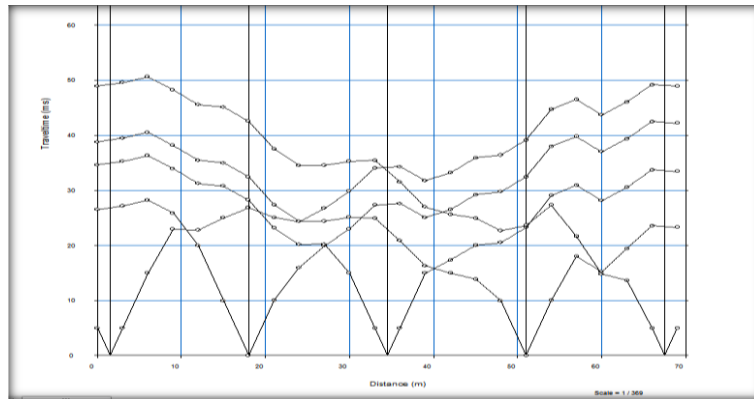


Fig. 9: Travel-Time Curve for Srt 4.

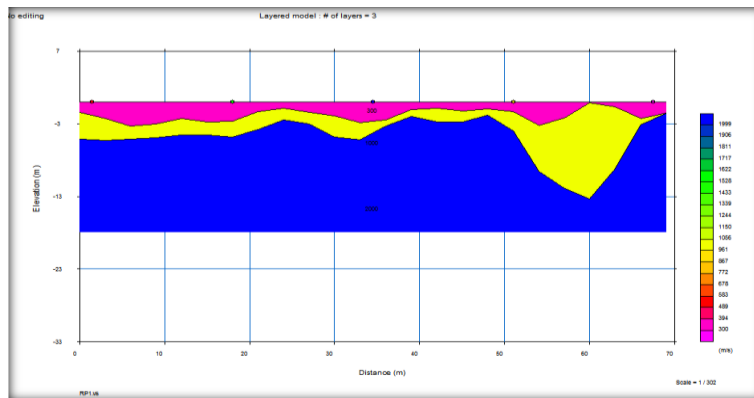


Fig. 10: Velocity Model for Srt 4.

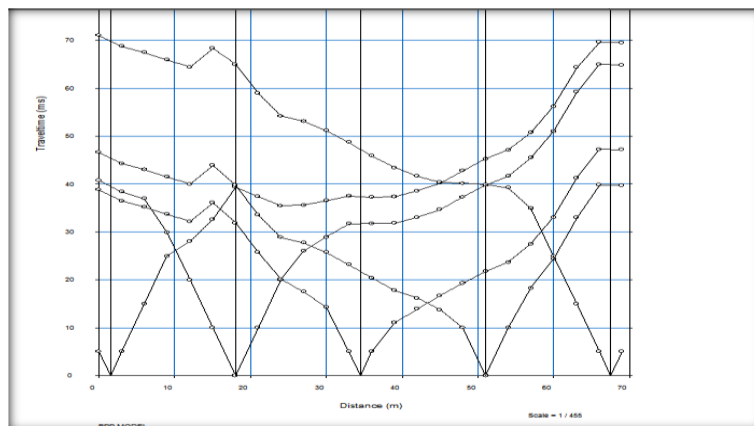


Fig. 11: Travel-Time Curve for Srt 5.

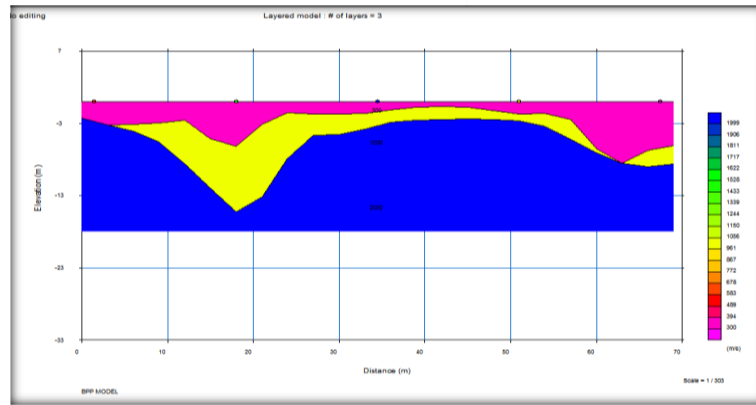


Fig. 12: Velocity Model for Srt 5.

The corresponding apparent resistivity pseudo sections for the four ERT profiles are presented in FIGs 13 – 16. Simultaneous iterated results were obtained for the same SRT profiles from the ERT data. ERT 1 revealed inverse modelled resistivity sections with values ranging from 2.23 Ωm to 826 Ωm with a suspected surface cave at a depth of approximately 12.5 m – 16.0 m with a resistivity value of 826 Ωm (FIG. 13). ERT 2 showed inverse modelled resistivity sections with values ranging from 12.8 Ωm to 120 Ωm with suspected caves at a depth of approximately 3.5 m – 9.3 m with resistivity values of approximately 53 Ωm – 120 Ωm (FIG. 14). ERT 3 revealed inverse modelled resistivity sections with resistivity values varying between 2.8 Ωm and 182 Ωm with suspected caves at resistivity sections with values of 116 Ωm and 182 Ωm at depths of approximately 3.5 m to 6.4 m and 4.0 m to 15.8 m respectively (FIG. 15). FIG. 16 shows inverse modelled resistivity sections for ERT 4 with resistivity values varying from 14.4 Ωm to 254 Ωm having a suspected cave at a resistivity section of 121 Ωm to 172 Ωm at a depth of approximately 9.5 m to 20.0 m which extends up to about 120.0 m from the edge of the highway (study area).

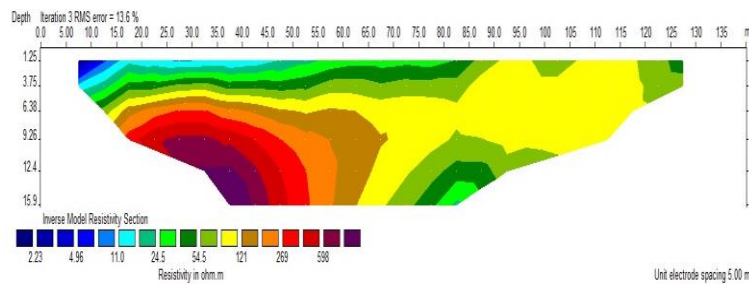


Fig. 2: Apparent Resistivity Model for Ert 1.

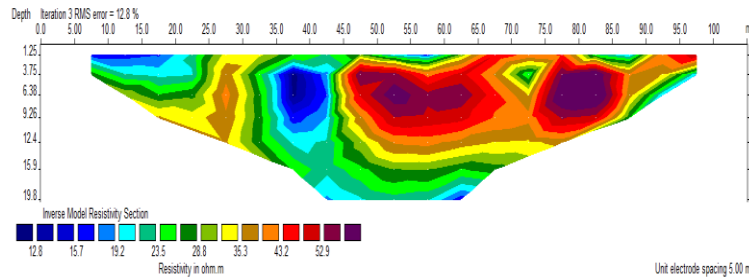


Fig. 14: Apparent Resistivity Model for Ert 2.

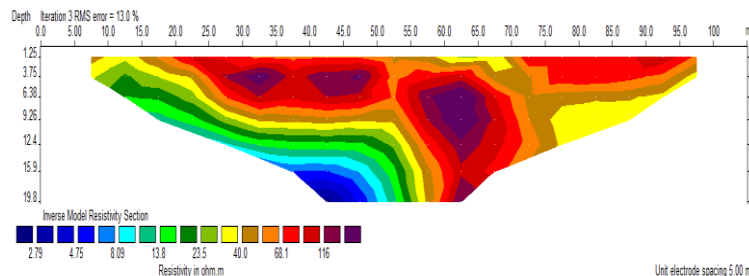


Fig. 15: Apparent Resistivity Model for Ert 3.

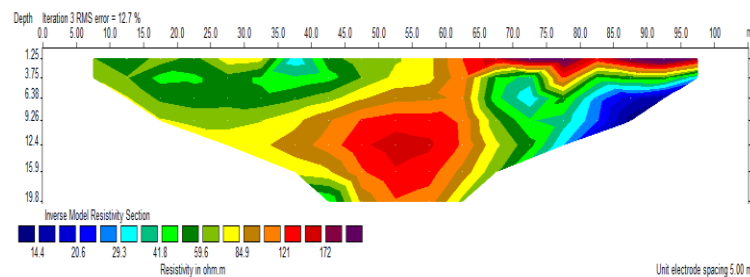


Fig. 16: Apparent Resistivity Model for Ert 4.

TABLE 2: Table Showing Geophysical Properties of Near-Surface Cavity in the Study Area

SRT Profile	ERT Profile	Cavity Layer	Modelled P-Wave Velocity (meters per second)	Mean Depth to Top Surface (meters)	Lateral Extension (meters)	Mean Apparent Resistivity (ohm-meter)	Depth to Top Surface (meters)	Lateral Extension (meters)
1	1	2	1,216	15.5	53.0	826	14.3	40.0
2	2	2	980	5.3	65.0	87	6.4	50.0
3	3	2	1,000	11.5	69.0	149	14.9	70.0
4	4	2	1,000	13.2	70.0	147	14.8	55.0
5	2	2	1,000	9.6	65.0			

4. Conclusion

Geophysical properties of near-surface cavities were determined in the Odukpani Central section of Calabar-Ikom Highway, Cross River State Nigeria. An integrated geophysical approach was employed for this study which comprised of SRT and Electrical ERT in an effort to complement the results of each geophysical technique.

Four to five survey lines/profiles were run for both the SRT and ERT measurements besides, opposite, and behind the near-surface cavity opening to determine the depth and lateral extensions of the suspected near-surface caves with prior consideration to the geology of the study area.

From the modelled velocity profiles for SRT 1 – 5, near surface caves were inferred on layer two at an approximate depth of 11.0 m – 20.0 m; layer two at an approximate depth of 3.5 m – 7.0 m, layer two at an approximate depth of 4.0 m – 7.0 m and 3.0 m – 9.0 m; layer two at an approximate depth of 0 m – 13.2 m; and layer two at an approximate depth of 6.0 m – 13.2 m respectively with all five layers having an average V_P of 1,039 ms^{-1} (TABLE 2).

In addition, near-surface cavities were detected in the study area which revealed apparent resistivity values of 826 Ωm for ERT 1, 87 Ωm for ERT 2, 149 Ωm for ERT 3, and 147 Ωm for ERT 4 (TABLE 2).

With the above observations, it is recommended amongst others that for the detected cavity which runs underneath the study area (as revealed by SRT and ERT profiles 2 and 3 respectively), the Government should commence an immediate mitigative construction (like installation of underground culverts/drainage) be carried out to forestall an impending ground surface subsidence of the study area (the Odukpani Central Section of Calabar-Ikom Highway).

Integration of two or more geophysical methods in the study of the earth's structure has always proved productive and resourceful because where one method is limited the other method compensates. This has been the case according to various related studies conducted by renowned geophysicists. Similar geophysical integration was carried out in this study, and the findings showed that the properties of near surface caves gotten from the seismic refraction tomography (SRT) measurements corresponded with the results gotten from electrical resistivity tomography (ERT) measurements.

Consequently, being that ERT profiles 2 and 3 (FIG. 14 and FIG. 15 respectively); and SRT profiles 2 and 3 (FIG. 6 and FIG. 8 respectively) mapped out the extension of the caves around the Odukpani Central section of Calabar-Ikom Highway, the findings inferred that the surface cave (that is already visible by the highway) extends laterally underneath and across the highway.

Recommendation is also made for the use of other geophysical techniques like Ground Penetration Radar (GPR) for further studies in conjunction to SRT and ERT to get higher resolution imagery of the study area.

Appendices

Appendix 1: Table of Profile Coordinates

S/N	SRT Profile	ERT Profile	Coordinates	Elevation (m)	Direction of Traverse	Traverse Length (M)
1.	SRT 1	ERT 1	N 05°08'273" E 008°20'572"	27.2	EW	69, 120
2.	SRT 2	ERT 2	N 05°08'285" E 008°20'575"	17.1	NS	69, 105
3.	SRT 3	ERT 3	N 05°08'192" E 008°20'344"	24.0	NS	69, 105
4.	SRT 4	ERT 4	N 05°08'173" E 008°20'389"	25.0	NS	69, 105
5.	SRT 5		N 05°08'173" E 008°20'389"	25.0	NS	69, 105

References

- [1] Adegbola, R. B., Ayolabi, E. A., & Allo, W. (2012). Subsurface Characterization using Seismic Refraction and Surface Wave Methods: A Case of Lagos State University, Ojo, Lagos State. *Arabian Journal of Geosciences*, 6(12), 4925-4930. <https://doi.org/10.1007/s12517-012-0784-2>.
- [2] Aderinola, O. S., & Onifade, S. O. (2004). Effect of the Cost of Bitumen and Bituminous Materials in Road Construction and Rehabilitation. *Copendum of Engineering Monograph*, 1(3), 1-7.
- [3] Adiat, K. A., Adelus, A. O., & Ayuk, M. A. (2009). Relevancy of Geophysics in Road Failures Investigation in a Typical Basement Complex of Southwestern Nigeria. *Pacific Journal of Science and Technology*, 5(1), 528-539.
- [4] Adiat, K. A., Akinlalu, A. A., & Adegoroye, A. A. (2017). Evaluation of Road Failure Vulnerability Section Through Integrated Geophysical and Geotechnical Studies. *NRIAG Journal of Astronomy and Geophysics*, 6, 244-255. <https://doi.org/10.1016/j.nrjag.2017.04.006>.
- [5] Ajayi, L. A. (1987). Thought on Road Failures in Nigeria. *Nigerian Eng.*, 22(1), 10-17.

- [6] Aka, M. U., Okeke, F. N., Ibout, J. C., & Obiora, D. N. (2018). Geotechnical Investigation of Near-Surface Structures Using Seismic Refraction Techniques in Parts of Akwa Ibom State. Southern Nigeria. *Modelling Earth Systems and Environment*, 4, 451-459. <https://doi.org/10.1007/s40808-018-0440-2>.
- [7] AL-Menshed, F. H. (2018). How to understand theoretical background of electrical resistivity in a simple way. Retrieved from Researchgate: <https://www.researchgate.net/publication/324747695>
- [8] Araffa, S. A., Atya, M. A., Mohamed, A. M., Gabala, M., Zaher, M. A., Soliman, M. M., . . . Shaaban, H. M. (2014). Subsurface investigation on Quarter 27 of May 15th city, Cairo, Egypt using electrical resistivity tomography and shallow seismic refraction techniques. *NRIAG Journal of Astronomy and Geophysics*, 3, pp 170-183. <https://doi.org/10.1016/j.nrjag.2014.10.004>.
- [9] ArcGIS (2016). Location Map of Odukpani. Esri. <https://www.arcgis.com/home/item.html>
- [10] Bery, A. A. (2013). High resolution in seismic refraction tomography for environmental study. *International Journal of Geosciences*, 4, pp. 792-796. <https://doi.org/10.4236/ijg.2013.44073>.
- [11] Bharti, A. K., Pal, S. K., Priyam, P., Kumar, S., Srivastava, S., & Yadav, P. K. (2016). Subsurface cavity detection over Patherdih colliery, Jharia Coalfield, India using electrical resistivity tomography. *Journal of Environmental Earth Science*, 75(443), 1-17. <https://doi.org/10.1007/s12665-015-5025-z>.
- [12] Burger, H. R., Sheehan, A. F., & Jon, C. H. (2006). *Introduction to Applied Geophysics: Exploring the Subsurface*. New York: W.W Norton.
- [13] Cardarelli, E., Cercato, M., Cerreto, A., & Di Filippo, G. (2010). Electrical resistivity and seismic refraction tomography to detect buried Cavities. *Geophysical Prospecting*, 58, 685-695. <https://doi.org/10.1111/j.1365-2478.2009.00854.x>.
- [14] Chalikakis, K., Plagnes, V., Guerin, R., Valois, R., & Bosch, F. (2011). Contribution of geophysical methods to karst-system exploration: An overview. *Hydrogeology Journal*, 19, 1169-1180. <https://doi.org/10.1007/s10040-011-0746-x>.
- [15] De Giorgi, L., & Leucci, G. (2014). Detection of Hazardous Cavities Below a Road Using Combined Geophysical Methods. *Survey Geophysics*. <https://doi.org/10.1007/s10712-013-9277-4>.
- [16] Everett, M. E. (2013). *Near-Surface Applied Geophysics*. UK: Cambridge University Press. <https://doi.org/10.1017/CBO9781139088435>.
- [17] Ilori, A. O. (2016). Occurrence of shale soils along the Calabar Itu highway, Southeastern Nigeria and their implication for the subgrade construction. *SpringerPlus*, 5(209), 1-13. <https://doi.org/10.1186/s40064-016-1822-4>.
- [18] Ilori, A. O., Obianwu, V. I. and Okwueze, E. E. (2014). Seismic Investigation of Highway Pavement Failures in Parts of Southeastern Nigeria. *Journal of Environmental and Engineering Geophysics*, 19(2), 113-134. <https://doi.org/10.2113/JEEG19.2.113>.
- [19] Jaafar, R. W. (2017). Imaging in karst terrain using the electrical resistivity and multi-channel analyses of surface wave methods. *Missouri: S & T Library and Learning Resources*. <https://doi.org/10.1190/segam2018-2998618.1>.
- [20] Khan, U., Niazi, A., & Basharat, M. (2018). Evaluating the Geological Structure of Landslides through Hydrogeological Modelling of Subsurface Sections, Using an Integrated Geophysical Approach. *Global Research and Development Journal for Engineering*, 3(12), 6-11.
- [21] Kim, J.-H., Yi, M.-J., Hwang, S.-H., Song, Y., Cho, S.-J., & Synn, J.-H. (2007). Integrated geophysical surveys for the safety evaluation of a ground subsidence in a small city. *Journal of Geophysics and Engineering*, 4, 332-347. <https://doi.org/10.1088/1742-2132/4/3/S12>.
- [22] Levik, K. (2002). How to sell the message 'Road Maintenance is Necessary to Decision Makers'. *Norwegian Public Road Administration*, pp. 1-4.
- [23] McNeill, J. D. (1980). *Electrical Conductivity of Soils and Rocks*. Technical Note: Geonics Limited. Ontario, Canada
- [24] Metwaly, M., & AlFouzan, F. (2013). Application of 2-D geoelectrical resistivity tomography for subsurface cavity detection in Saudi Arabi. *Geoscience Frontiers*(4), 469-476. <https://doi.org/10.1016/j.gsf.2012.12.005>.
- [25] NPC. (2006). *Population of Cross River State*. Abuja: National Population Commission. Retrieved from <http://www.nigerianstat.gov.ng>
- [26] Nwosu, L. I., & Emujakporue, G. O. (2016). Seismic Refraction Investigation of Thickness and Velocity of the Weathered Layer in Emuoha Town, Rivers State, Nigeria. *IOSR Journal of Applied Geology and Geophysics*, 4(6), 52-57.
- [27] Obianwu, V. I., Udoh, J. T., George, A. M., & George, N. J. (2015). Seismic Early Warning Foundation Conditions Evaluation Survey for Civil Engineering Constructions in Akpabuyo Local Government Area of Cross River State, Nigeria. *British Journal of Applied Science & Technology*, 6(6), 583-596. <https://doi.org/10.9734/BJAST/2015/14930>.
- [28] Okigbo, N. (2017). Causes of Highway Failures in Nigeria. *Internationa; Journal of Engineering Science and Technology*, 4696-4697.
- [29] Olson Engineering. (2021). *Seismic Refraction Tomography*. Retrieved from Olson Engineering: <http://www.olsonengineering.com/methods/geophysical-methods/seismic/refraction-srt/>. Date Retrieved: November 15, 2021.
- [30] Petters, S. W., Nyong, E. E., Akpan, E. B., & Essien, N. U. (1995). Litho-stratigraphic revision of the Calabar Flank, S. E. Nigeria. *Proceedings of the 31st anniversary conference of Nigeria Mining and Geosciences Society*, 57, pp. 755-760. Calabar: Planets Space.
- [31] Putiška, R., Kušniřák, D., Dostál, I., Lačný, A., Mořez, A., Hók, J., . . . Bořanský, M. (2014). Integrated Geophysical and Geological Investigation of Karst Structures in Kombat, Slovakia. *Journal of Cave and Karst Studies*, 76(3), 155-165. <https://doi.org/10.4311/2013ES0112>.
- [32] Reymont, R. A. (1965). *Aspects of the geology of Nigeria*. Ibadan: Ibadan University Press.
- [33] Rodríguez, J. A., Flores, M. A., Carmentales, Y. A., & Hernández, M. B. (2020). Electrical Resistivity Tomography for the detection of subsurface cavities and related hazards caused by underground coal mining in Coahuila. *Geofísica internacional*, 58(4). <https://doi.org/10.22201/igeof.00167169p.2019.58.4.2058>.
- [34] Samyn, K., Mathieu, F., Bitri, A., Nachbaur, A., & Closser, L. (2014). Integrated geophysical approach in assessing karst presence and sinkhole susceptibility along flood-protection dykes of the Loire River, Orleans, France. *Engineering Geology*, 183, 170-184. <https://doi.org/10.1016/j.enggeo.2014.10.013>.
- [35] Senkaya, G. V., Senkaya, M., Karsli, & Güney, R. (2020). Integrated shallow seismic imaging of a settlement located in a historical landslide area. *Bulletin of Engineering Geology and the Environment*, 79, 1781-1796. <https://doi.org/10.1007/s10064-019-01612-0>.
- [36] Shaaban, F., Ismail, A., Massoud, U., Mesbah, H., Lethy, A., & Abbas, A. M. (2013). Geotechnical assessment of ground conditions around a tilted building in Cairo-Egypt using geophysical approaches. *Journal of Association of Arab Universities for Basic and Applied Sciences*, 13, 63-72. <https://doi.org/10.1016/j.jaubas.2012.06.002>.
- [37] Shehu, A. D., Abdulrahman, A., & George, V. E. (2016). Assessment of the extent of soil corrosivity using vertical electrical sounding: a case study of Mbat-Odukpani, Cross River, Nigeria. *Journal of League of Researchers in Nigeria*, 17(1), 1-10.
- [38] United States Bureau of Reclamation (USBR) (2002). *Engineering Geology Field Manual*. 2nd Ed. II.
- [39] Akakuru O.C, Adakwa C.B, Ikoro D.O, Eyankware M.O, Opara A.I, Njoku A.O, Iheme K.O, Usman A.O (2023a). Application of Artificial Neural Network and Multi-linear Regression Techniques in Groundwater Quality and Health Risk Assessment around Egbema, Southeastern Nigeria. *Environmental Earth Science*. <https://doi.org/10.1007/s12665-023-10753-1>
- [40] Akakuru, O.C., Opara, A.I., Aigbadon, G.O. et al. Characterizing gully-prone zones using geophysical and geotechnical approaches: a case study of Njaba South-Eastern Nigeria. *Int. J. Environ. Sci. Technol.* (2023b). <https://doi.org/10.1007/s13762-023-05301-0>
- [41] Akakuru O.C, Njoku B.U, Obinna-Akakuru A.U, Akudinobi B E.B, Obasi P N, Aigbadon G.O, Onyeawuna U.B (2023c). Non-carcinogenic Health Risk Assessment and Prediction of Organic and Heavy Metal Pollution of Groundwater around Osioma, Nigeria, using Artificial Neural Networks and Multi-Linear Modeling Principles. *Stochastic Environmental Research and Risk Assessment* 10.1007/s00477-023-02398-0
- [42] Eyankware, M.O., Akakuru, O.C., Osisanya, W.O. et al. Assessment of heavy metal pollution on groundwater quality in the Niger Delta Region of Nigeria. *Sustain. Water Resour. Manag.* 9, 189 (2023). <https://doi.org/10.1007/s40899-023-00955-7>
- [43] Chizoba, J. C., Usman, A. O., Ezech, C. C., Chinwuko, I. A., Azuoko, G. B., Akakuru, O. C., & Iheme, K. O. (2023). Hydrogeological assessment of groundwater resources within Isuikwuato and environs Southeastern Nigeria: Agenda for food agriculture and clean water policies. *International Journal of Physical Sciences*, 18
- [44] Alexander Iheanyichukwu Opara, Anita Nneoma Ireaja ., Moses Oghenyoreme Eyankware, Obinna Oko Urom, Diogu Okereke Ikoro, Obinna Chigoziem Akakuru, Emmanuel Dioha and Newton Ejiro Omoko (2023). Comparative analysis of techniques used for aquifer protective capacity studies in the Southeastern part of Nigeria. *International Journal of Energy and Water*. 10.1007/s42108-023-00251-2

- [45] Omoko, Ejiro Newton., Opara, Alexander Iheanyichukwu., Onyekuru, Samuel Okechukwu., Ibeneme, Sabinus Ikechukwu., Akakuru, Obinna Chigoziem and Fagorite, Victor Immuden (2023). Pollution status and hydrogeochemical characterization of water resources in Onne industrial layout and environs, Rivers state, Nigeria. *Sustainable Water Resources Management*. 10.1007/s40899-023-00886-3
- [46] Akakuru O.C, Akaolisa C.C.Z, Aigbadon G.O, Eyankware M.O, Opara A.I, Obasi P.N, Ofoh I.J, Njoku A.O, Akudinobi, B.E.B(2022a). Integrating machine learning and multi-linear regression modeling approaches in groundwater quality assessment around Obosi, SE Nigeria. *Environment, Development and Sustainability*. 10.1007/s10668-022-02679-8 (Springer).
- [47] Akakuru, O.C, Eze, C.U., Okeke, O.C, Opara A.I., Usman, A.O., IHEME O.K, Ibeneme, S.I, & Iwuoha, P.O (2022b). Hydrogeochemical evolution, water quality indices, irrigation suitability and pollution index of groundwater (PIG) around Eastern Niger Delta, Nigeria. *International Journal of Energy and Water Resources*. <https://doi.org/10.1007/s42108-021-00162-0>
- [48] Agidi, B.M., Akakuru, O.C., Aigbadon, G.O. Schoeneich K., Isreal H, Ofoh I, Njoku J, Esomonu I (2022). Water quality index, hydrogeochemical facies and pollution index of groundwater around Middle Benue Trough, Nigeria. *International Journal of Energy and Water Resources*. <https://doi.org/10.1007/s42108-022-00187-z>
- [49] Eyankware, M.O, Akakuru, O.C, Eyankware E.O (2022a). Interpretation of hydrochemical data using various geochemical models: a case study of Enyigba mining district of Abakaliki, Ebonyi State, SE Nigeria. *Sustainable Water Resources Management*. <https://doi.org/10.1007/s40899-022-00613-4>
- [50] Eyankware, M.O., Akakuru, O.C. (2022). Appraisal of groundwater to risk contamination near an abandoned limestone quarry pit in Nkalagu, Nigeria, using enrichment factor and statistical approaches. *International Journal of Energy and Water Resources*. <https://doi.org/10.1007/s42108-022-00186-0>
- [51] Alexander Iheanyichukwu Opara, Osi-Okeke, Ifeanyi Edward., Moses Oghenenyoreme Eyankware., Obinna Chigoziem Akakuru., Ifeanyi Chidozie Oli and Harry Moses Udeh (2022). Use of geo-electric data in the determination of groundwater potentials and vulnerability mapping in the southern Benue Trough Nigeria. *International Journal of Environmental Science and Technology*. 10.1007/s13762-022-04485-1
- [52] Oli, I.C., Opara, A.I., Okeke, O.C. Akaolisa C.Z, Akakuru, O.C, Osi-Okeke I, Udeh H.M (2022). Evaluation of aquifer hydraulic conductivity and transmissivity of Ezza/Ikwo area, Southeastern Nigeria, using pumping test and surficial resistivity techniques. *Environ Monit Assess* 194, 719. <https://doi.org/10.1007/s10661-022-10341-z>
- [53] Eyankware M.O, Akakuru O.C, Ulakpa, R.O. E and Eyankware E.O (2022b) Hydrogeochemical approach in the assessment of coastal aquifer for domestic, industrial, and agricultural utilities in Port Harcourt urban, Southern Nigeria. *International Journal of Energy and Water Resources*. <https://doi.org/10.1007/s42108-022-00184-2>
- [54] Obasi, P.N. ; Akakuru, O.C. , Nweke, O.M. and Okolo C.M (2022). Groundwater assessment and contaminant migration in fractured shale aquifers of Abakaliki mining areas, Southeast Nigeria. *Journal of Mining and Geology*. 58(1), 211 – 227
- [55] Moses Oghenenyoreme Eyankware, Obinna Chigoziem Akakuru, Emmanuel Oghenegare Eyankware, Ezekiel Obinna Igwe, Star Otitie Umayah (2022c). Modeling approach to the investigation of groundwater corrosion and scaling potential at Benue State, Nigeria. *World Scientific News* 172. 179-212
- [56] Obasi, P.N., Ani, C.C, Akakuru, O.C. & Akpa, C (2020). Determination of Aquifer Depth Using Vertical Electrical Sounding in Ihechiowa Area, Arochukwu Southeast Nigeria. *EBSU Science Journal*, 1(1), 111 – 126
- [57] ssUrom, O.O., Opara, A.I., Usen, O.S., Akiang, F.B., Isreal, H.O., Ibezim, J.O. & Akakuru, O.C. (2021). Electro-geohydraulic estimation of shallow aquifers of Owerri and environs, Southeastern Nigeria using multiple empirical resistivity equations. *International Journal of Energy and Water Resources*, 1-22. <https://doi.org/10.1007/s42108-021-00122-8>